Antisense PMO Found in Dystrophic Dog Model Was Effective in Cells from Exon 7-Deleted DMD Patient

Takashi Saito[1,2], Akinori Nakamura[1], Yoshitsugu Aoki[1], Toshifumi Yokota[3], Takashi Okada[1], Makiko Osawa[2], Shin'ichi Takeda[1]*

1 Department of Molecular Therapy, National Institute of Neuroscience, National Center of Neurology and Psychiatry, Kodaira, Tokyo, Japan, 2 Department of Pediatrics, School of Medicine, Tokyo Women's Medical University, Shinjuku, Tokyo, Japan, 3 Research Center for Genetic Medicine, Children's National Medical Center, Washington, District of Columbia, United States of America

Abstract

Background: Antisense oligonucleotide-induced exon skipping is a promising approach for treatment of Duchenne muscular dystrophy (DMD). We have systemically administered an antisense phosphorodiamidate morpholino oligomer (PMO) targeting dystrophin exons 6 and 8 to a dog with canine X-linked muscular dystrophy in Japan ($CXMD_J$) lacking exon 7 and achieved recovery of dystrophin in skeletal muscle. To date, however, antisense chemical compounds used in DMD animal models have not been directly applied to a DMD patient having the same type of exon deletion. We recently identified a DMD patient with an exon 7 deletion and tried direct translation of the antisense PMO used in dog models to the DMD patient's cells.

Methodology/Principal Findings: We converted fibroblasts of CXMD, and the DMD patient to myotubes by FACS-aided MyoD transduction. Antisense PMOs targeting identical regions of dog and human dystrophin exons 6 and 8 were designed. These antisense PMOs were mixed and administered as a cocktail to either dog or human cells *in vitro*. In the $CXMD_J$ and human DMD cells, we observed a similar efficacy of skipping of exons 6 and 8 and a similar extent of dystrophin protein recovery. The accompanying skipping of exon 9, which did not alter the reading frame, was different between cells of these two species.

Conclusion/Significance: Antisense PMOs, the effectiveness of which has been demonstrated in a dog model, achieved multi-exon skipping of dystrophin gene on the FACS-aided MyoD-transduced fibroblasts from an exon 7-deleted DMD patient, suggesting the feasibility of systemic multi-exon skipping in humans.

Citation: Saito T, Nakamura A, Aoki Y, Yokota T, Okada T, et al. (2010) Antisense PMO Found in Dystrophic Dog Model Was Effective in Cells from Exon 7-Deleted DMD Patient. PLoS ONE 5(8): e12239. doi:10.1371/journal.pone.0012239

Editor: Antoni L. Andreu, Hospital Vall d'Hebron, Spain

Received May 7, 2010; **Accepted** July 21, 2010; **Published** August 18, 2010

Funding: This work was supported by the Health and Labour Sciences Research Grants for Translational Research from the Ministry of Health, Labour and Welfare of Japan (H19-Translational Research-003, H21-Translational Research-011, H21-Clinical Research-011). The funders had no role in study design, data collection and analysis, decision to publish, or preparation of the manuscript.

Competing Interests: The authors have declared that no competing interests exist.

* E-mail: takeda@ncnp.go.jp

Introduction

Antisense oligonucleotides (AON) have been reported to modulate splicing of pre-mRNA transcribed from mutated genes and to restore a normal reading frame in several diseases. Duchenne muscular dystrophy (DMD), a degenerative muscle disorder caused mainly by nonsense or frame-shift mutations of the dystrophin gene, is one of the diseases that could be treated by AON-mediated exon skipping. Previously reported studies were conducted *in vitro*, in animal models, and as patient intervention studies, and they showed restorations of the reading frame in dystrophin mRNA and recoveries of dystrophin protein expression [1,2,3]. Among the several AON chemistries that have been introduced thus far, a phosphorodiamidate morpholino oligomer (PMO) and 2'-O-methyl phosphorothioate (2'OMe) oligomer are promising candidates owing to their stabilities and efficacies, and they are now undergoing phase I-II clinical trials in the United Kingdom and the Netherlands, respectively [4,5]. The AON-mediated exon skipping is already in a late early stage of clinical application; therefore, it is rational to translate pre-clinical animal model knowledge into a patient-based study.

We have previously reported that the systemic administration of an antisense PMO for canine X-linked muscular dystrophy in Japan ($CXMD_J$) achieved restoration of dystrophin and amelioration of symptoms [6]. $CXMD_J$ harbors a splice site mutation within the splice acceptor site of intron 6 of the dystrophin gene. The mutation disrupts the splicing of exon 7, and thus the dystrophin mRNA lacks exon 7 [7]. In $CXMD_J$, multiple skipping of exons 6 and 8 restores the reading frame, and the multi-exon skipping approach is expected to expand the number of DMD cases potentially treatable by exon skipping [8]. $CXMD_J$ is an ideal model of multi-exon skipping, and we hope to translate the results to human patients. However, in the road to ongoing clinical trials, *in vitro* assays on patient cells are indispensable.

To date, antisense sequences used for exon skipping in DMD animal models have not been directly applied to a DMD patient having the same type of exon deletion. We identified an exon 7-deleted patient (referred to as DMD 8772) and tried direct

translation of the antisense PMO design from a DMD dog model to the DMD patient. We tried *in vitro* multi-exon skipping with the same antisense PMO that was used in $CXMD_J$ in the patient's cells before attempting delivery of the PMO into the patient.

Which cells should be used for *in vitro* dystrophin exon skipping is controversial. Myoblasts are usually employed simply because they express enough dystrophin as mRNA and protein, but collecting them requires an invasive muscle biopsy. In cases where myoblasts were not available, it had been reported that the dystrophin mRNA was detected in lymphocytes and fibroblasts by nested RT-PCR. Some studies actually demonstrated the success of exon skipping in mRNA of lymphoblastoid cells and fibroblasts [9,10], but the restoration of dystrophin protein could not be analyzed in these cells because their transcripts were illegitimate and too low to be translated into gene products [11]. As another alternative, fibroblasts are converted to myotubes by MyoD transduction [4,12,13]. Transduced cells express dystrophin mRNA and protein, but achievement of sufficient protein expression is challenging [14,15,16]. In this study, we addressed this issue by introducing a retroviral vector co-expressing MyoD and green fluorescent protein (GFP) and flow cytometry, and then quantified the dystrophin expression of the cells to evaluate the feasibility of exon skipping.

We first report multiple skipping of dystrophin exons 6 and 8 in the DMD patient's cells and translation of the unified antisense PMO design from a DMD dog model to a human based on the MyoD-transduction method utilizing flow cytometry.

Results

Mutation analysis of DMD 8772

DMD 8772, a 22-year-old man, manifested severe muscle weakness, wheelchair dependency, and mild cardiac dysfunction. No evidence of dystrophin protein had been observed on a previous muscle biopsy, and the patient had been diagnosed with a frame-shift deletion of dystrophin exon 7 by multiplex ligation-dependent probe amplification (MLPA) analysis. The deletion of exon 7 leads to a premature translation termination at exon 8. The deletion of exon 9 is known as a common splice variant maintaining the reading frame in dogs and humans [17,18] (**Figure 1A**). RT-PCR analysis of dystrophin mRNA using the patient's lymphocytes showed an exon 7 deletion, and direct sequence analysis of the RT-PCR products revealed a conjunction of exons 6 and 8 (**Figure 1B**). To determine the intron length, we performed a deletion breakpoint analysis. The genomic PCR roughly narrowed the breakpoint window to 2.5 kb between introns 6 and 7, then primer walking sequence analysis revealed the 50.4 kb deletion (Vega v35 chromosome X 32771568 to 32821979) [13] and the breakpoint accompanying an insertion of 13 bases of unknown origin (**Figure 1C**).

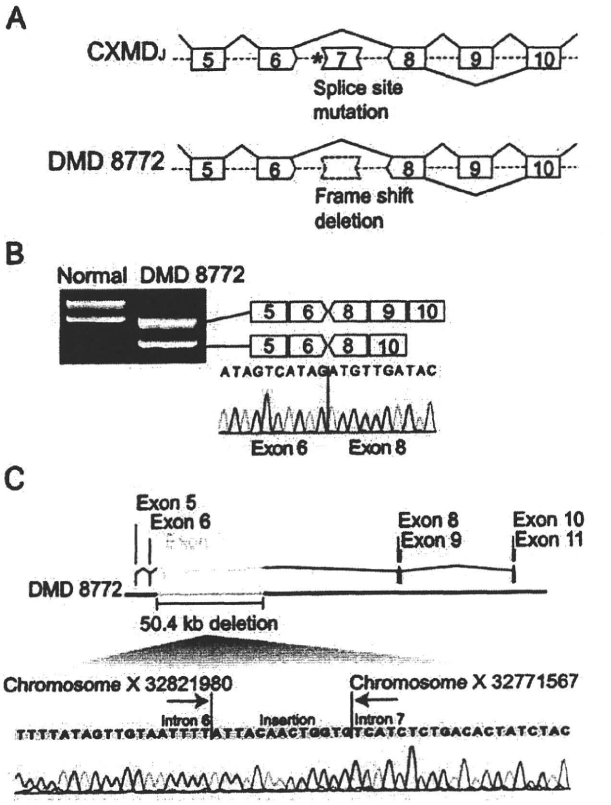

Figure 1. Mutation analysis of DMD 8772. (A) Splice-site mutation of a splice acceptor site in intron 6 (asterisk) excludes exon 7 from dog dystrophin mRNA. Frame-shift deletion of dystrophin exon 7 in DMD 8772 was diagnosed by MLPA analysis. Skipping of exon 9 is a frequent splice variant. Both ends of the schematic box of the exon represent a phase of the codon (see detail, Yokota et al. 2009). (B) RT-PCR and sequence analysis of dystrophin mRNA using normal and DMD 8772 lymphocytes. Double bands due to a splicing variant of exon 9 were observed. (C) Breakpoint analysis of DMD 8772 revealed a 50.4 kb deletion from intron 6 to intron 7, and the insertion of 13 bases of unknown origin.
doi:10.1371/journal.pone.0012239.g001

Myogenic conversion of fibroblasts by MyoD transduction and selection of appropriate cell lineage for exon skipping

We prepared lymphoblastoid cells, fibroblasts, and MyoD-transduced fibroblasts from DMD 8772 and assessed the feasibility of exon skipping in these cells. To establish MyoD-transduced fibroblasts, primary fibroblasts were transfected by a retrovirus encoding murine or human MyoD and GFP with the vesicular stomatitis virus (VSV-G) envelope through standard procedures (**Figure 2A**) [19,20]. To compare exon skipping between corresponding cells of $CXMD_J$ and DMD 8772, fibroblasts from both were converted. In addition, normal dog and human fibroblasts were also transduced for evaluation. After virus transfection, we sorted GFP-positive cells by flow cytometry. The ratio of GFP-positive to -negative cells was dependent on cell lineage, and affected cells generally showed lower transfection efficiencies (**Figure 2B**). The GFP-positive cells were isolated in serum-deprived medium for myogenic differentiation and cultured for 10 to 16 days. We confirmed that the cultured cells had the morphological features of myotubes of multiple nuclei and longitudinal growth. Immunostaining analysis showed nuclear localization of MyoD and expressions of the muscle-specific proteins desmin, myosin heavy chain, and dystrophin (**Figure 2C**). Using normal dog and human fibroblasts, we performed time-course expression analyses of dystrophin mRNA by qRT-PCR and dystrophin protein by Western blot. The results showed a gradual increase in dystrophin expression. In dog cells, dystrophin became detectable on the protein level seven days after differentiation, whereas human cells required two weeks or more (**Figure 2D**). We compared the dystrophin mRNA expression of the lymphoblastoid cells, fibroblasts, and MyoD-transduced fibroblasts from DMD 8772. The MyoD-transduced fibroblasts showed remarkable expression compared with the other cells (**Figure 2E**). We tried exon skipping in lymphoblastoid cells, fibroblasts and MyoD-transduced fibroblasts, but only the MyoD-transduced

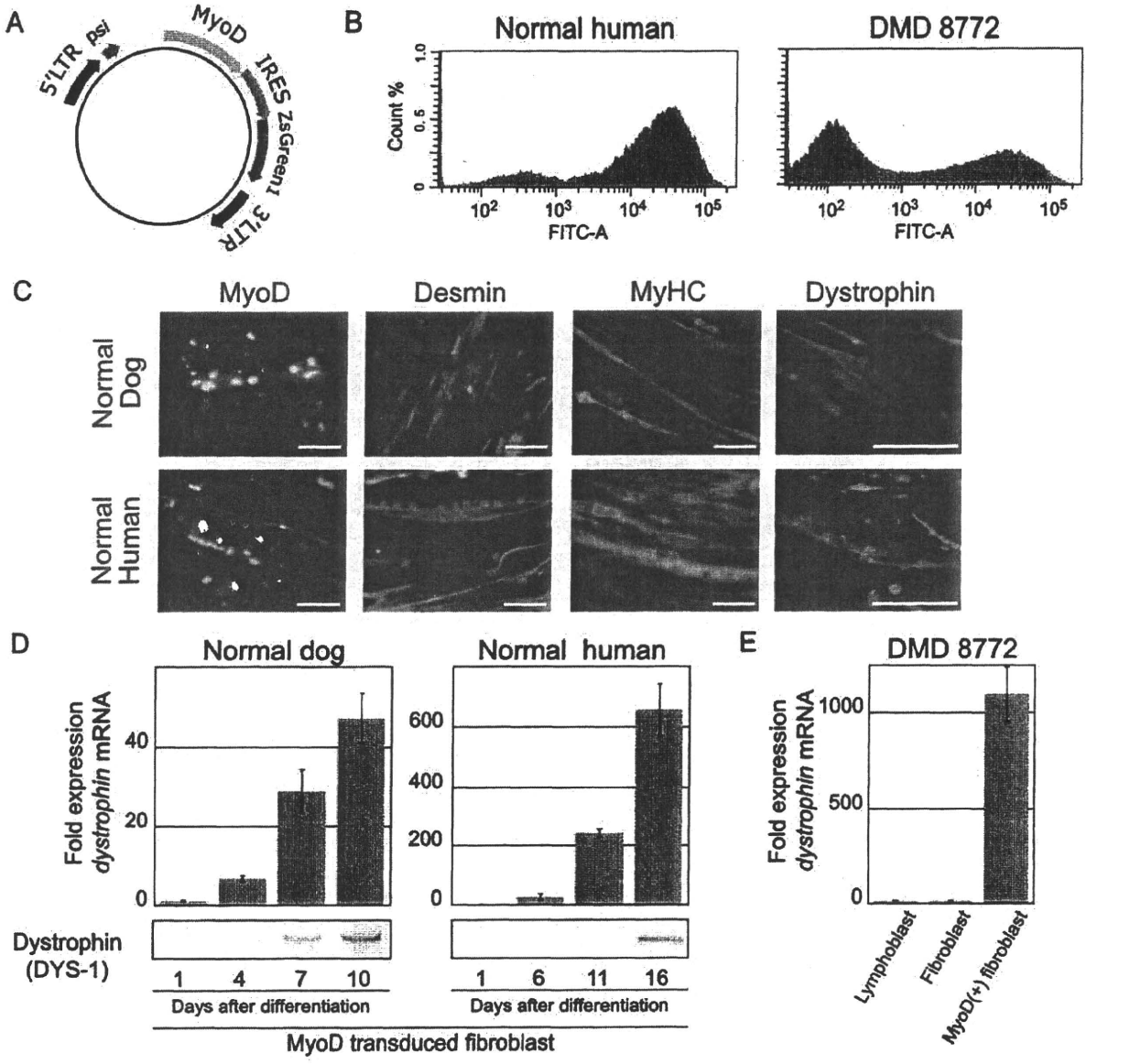

Figure 2. Myogenic conversion of fibroblasts and dystrophin expression. (A) Schematic diagram of the retroviral expression vector. (B) Histograms showing GFP fluorescence intensity compared with cell numbers of normal human and DMD 8772 MyoD-GFP-transduced fibroblasts. Both cells were analyzed five days after retroviral transfection. (C) Immunostaining of MyoD-transduced of dog and human fibroblasts after 10 and 15 days of myogenic differentiation, respectively. MyHC, myosin heavy chain. The nuclei were counter-stained with DAPI. Scale bar: 100 μm. (D) The time course of dystrophin expression in dog and human MyoD-transduced fibroblasts by qRT-PCR and immunoblotting analysis. The mRNA levels were normalized to *GAPDH* and expressed relative to the amount of the lowest one in each group. For immunoblotting, 5 μg of total protein was loaded into each lane. Error bars indicate standard deviation. (E) Determination of dystrophin mRNA expression in each cell type from DMD 8772 by qRT-PCR. MyoD-transduced fibroblasts were assayed 15 days after differentiation. Normalization and relative expression are the same as (D).
doi:10.1371/journal.pone.0012239.g002

fibroblasts yielded reproducible results. The lymphoblastoid cells and fibroblasts often failed to produce PCR products, and the skipped in-frame products were undetectable even if PCR products were generated (**data not shown**). Therefore, we used MyoD-transduced fibroblasts in the subsequent assays.

Antisense PMO sequence design

In a previous systemic dog study, we used three antisense sequences, Ex6A, Ex6B, and Ex8A, as three antisense PMO cocktails [6]. Because there were two base mismatches between dog and human Ex6B, hEx6B was newly designed on the identical region of Ex6B, modifying the mismatches of the human sequence. In the systemic study, we skipped exon 6 with a combination of Ex6A and Ex6B, and thus we tried same strategy for exon 8. We newly designed several antisense PMOs targeting exon 8 that were positioned on the identical sequence in dog and human considering the predicted *in silico* splice-enhancer motifs (**Figure 3A**). A preliminary assay of $CXMD_J$ cells showed that three sequences, Ex8G, Ex8I, and Ex8K, were effective. Therefore, the antisense combination for exon 8 contained an extra antisense sequence

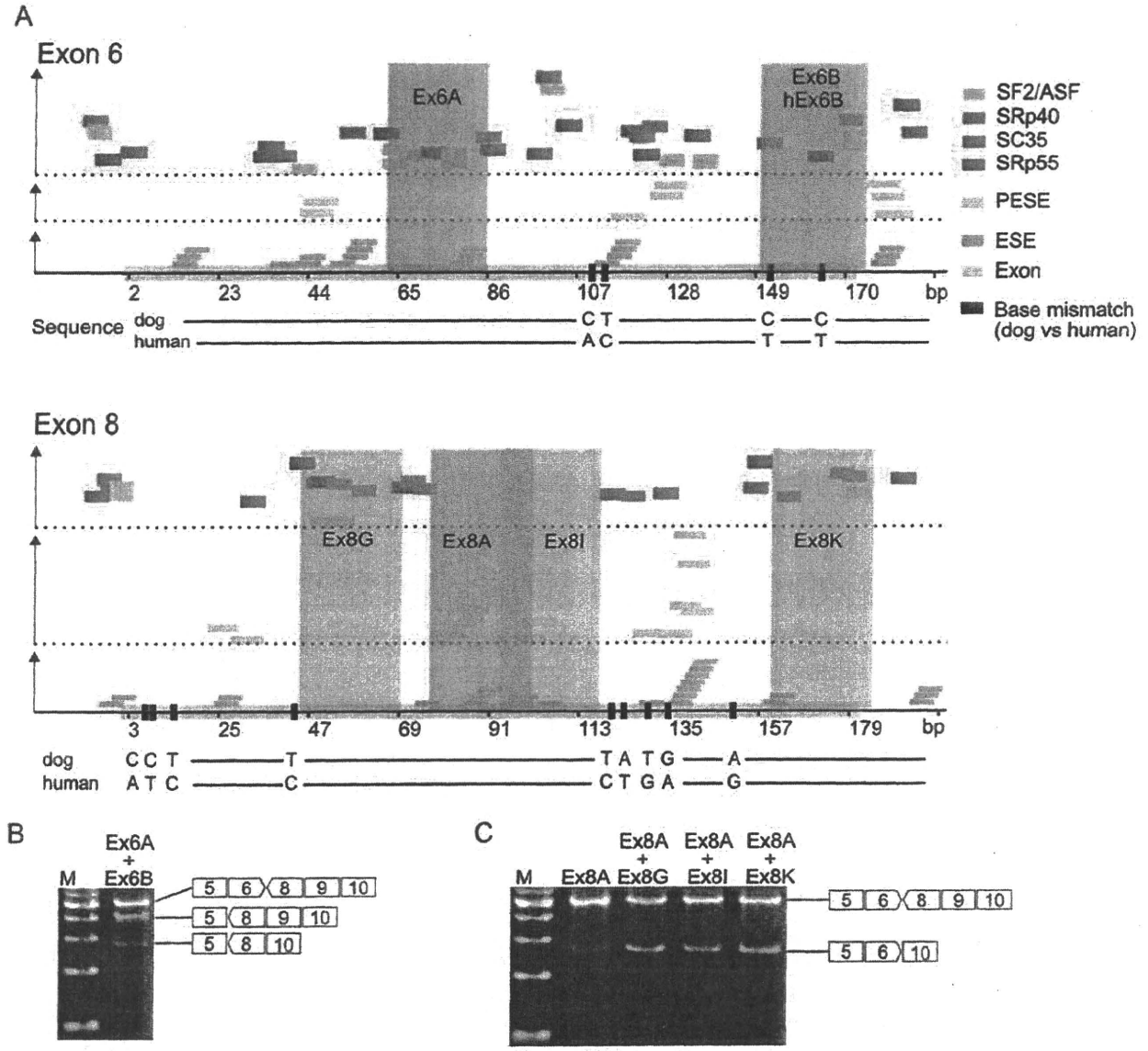

Figure 3. Design of antisense PMO sequence targeting exons 6 and 8. (A) Exonic splicing enhancer motifs predicted *in silico* based on human sequence (small coloured boxes) and positions of antisense PMOs (green and blue rectangular areas). The horizontal axis represents base positions in each exon from 5′ to 3′, and the vertical axis represents relative predicted values of the motifs. PESE: putative exonic splicing enhancer. ESE: exonic splicing enhancer. Base mismatches between dog and human (black bar) are indicated in the exon (grey box). RT-PCR of dystrophin mRNA of MyoD-transduced CXMD$_J$ fibroblasts treated with (B) a mixture of Ex6A and Ex6B and (C) only Ex8A or mixtures containing Ex8A.
doi:10.1371/journal.pone.0012239.g003

from Ex8G, Ex8I, or Ex8K in addition to that of Ex8A. The skipping efficacy of each combination was higher than that of Ex8A alone, and those of Ex8G, Ex8I, and Ex8K were comparable (**Figure 3C**).

Comparison of multiple skipping of exons 6 and 8 between CXMD$_J$ and DMD 8772 cells

The multi-exon skipping of exons 6 and 8 employed three- and four-antisense PMO cocktails. In the three-antisense PMO cocktail for dogs, Ex6A, Ex6B, and Ex8A were included, and Ex6B was replaced with hEx6B for the human. The four-antisense PMO cocktail included one of Ex8G, Ex8I, or Ex8K in addition to the three-antisense PMO cocktail (**Figure 4A**). When we transfected the three- or four-antisense PMO cocktails into the MyoD-transduced fibroblasts, we did not observe the skipped products (231 bp) of exons 6-8 on RT-PCR analyses of CXMD$_J$ but did observe the skipped products (99 bp) of exons 6-9. A sequence analysis also confirmed the concatenation of exons 5 and 10. In DMD 8772, we observed skipped products (221 bp and 92 bp, respectively) of both exons 6-8 and exons 6-9. Sequence analysis also showed that the skipped products were concatenations of exons 5 to 9 and exons 5 to 10. The four-PMO cocktails produced more in-frame products than the three-PMO cocktail, but we discerned no difference among the four PMO cocktails. This tendency was also consistent between CXMD$_J$ and DMD 8772 (**Figure 4B**). Immunostaining analysis showed partial recovery of dystrophin in the four-antisense PMO

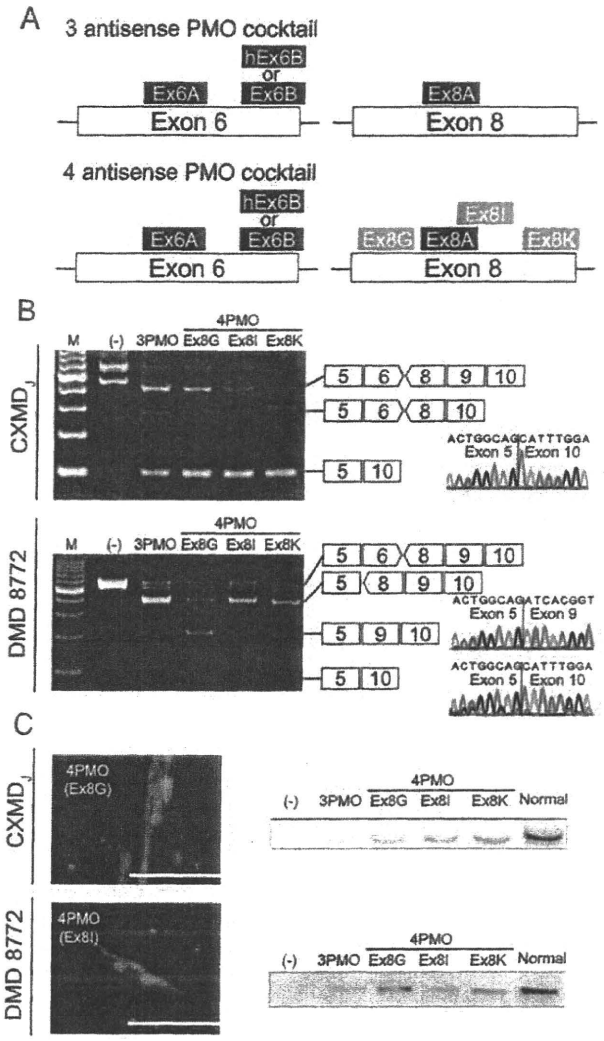

Figure 4. Multi exon skipping and recovery of dystrophin in CXMD$_J$ and DMD 8772-derived cells. (A) Schematic diagram of the three- and four-antisense PMO cocktails. For DMD 8772, Ex6B was replaced with hEx6B. In the four-antisense PMO cocktail, one additional sequence (Ex8G, Ex8I, or Ex8K) was added to the three-antisense PMO cocktail. (B) RT-PCR of dystrophin mRNA isolated from MyoD-transduced fibroblasts after treatment with the three- and four-antisense PMO cocktails. In-frame exon skipping products were 99 bp in dog and 221 bp and 92 bp in human. (C) Representative immunostaining and immunoblotting analysis of MyoD-transduced fibroblasts treated with antisense PMO cocktails. The nuclei were counterstained with DAPI. Scale bar: 100 μm. Expected molecular weights of truncated human dystrophin with exons 6–8 and exons 6–9 skipped are 18.3 kDa and 23.1 kDa, respectively, smaller than the full-length dystrophin.
doi:10.1371/journal.pone.0012239.g004

cocktail-treated cells without obvious differences between them (**Figure 4C**). Western blots of dystrophin showed products that were slightly smaller than the full-length dystrophin. In RT-PCR of DMD 8772, skipped mRNA of both exons 6-8 and 6-9 were detected; however, distinguishing the truncated dystrophins translated from these mRNA variants was impossible. Similar to the RT-PCR results, the dystrophin expression level was higher with a four-PMO cocktail than with the three-PMO cocktail. Differences between the four-PMO cocktails were also undetectable.

Discussion

In this study, we accomplished *in vitro* multi-exon skipping in a DMD patient carrying the same deletion as CXMD$_J$ by using the identical antisense PMO. We also addressed the efficient MyoD transduction of fibroblasts with FACS, and discuss the difference of the spliced exon associated with it with the frequency of alternative splicing.

FACS-aided MyoD transduction provided sufficient dystrophin expression

We evaluated the appropriateness of lymphoblastoid cells, fibroblasts, and MyoD-transduced fibroblasts as an alternative to myoblasts for exon-skipping assays. Lymphoblastoid cells and primary fibroblasts dystrophin mRNA required reamplification by nested RT-PCR [9,10], and the results were not reproducible, suggesting that low dystrophin expression may hamper reliable quantitative assessments. Only MyoD-transduced fibroblasts showed reproducible results due to their stable dystrophin expression. We employed flow cytometry for selection of MyoD-positive cells; it seems to offer several advantages against conventional drug-resistance selection. First, the transfection ratio in drug-resistance selection remains unknown until a selective drug is added. In contrast, with MyoD-transduced fibroblasts, we were able to roughly determine the ratio by fluorescence microscopy and adjust the culture scale to meet the size of the assay. Second, a low rate of myotubes formation after drug-resistance selection has been reported [21]. Our method actively selects MyoD-positive cells and enables pure clusters of MyoD-positive cells to form myotubes efficiently. MyoD transduction with GFP has been reported in several studies [22,23] but not in dystrophin exon-skipping studies. We demonstrated that it is a suitable approach for the exon-skipping assay here as well. Several studies have reported difficulties inducing dystrophin in human cells with MyoD transduction [14,15,16]. In our experience, the typical morphological features of myotubes, multiple nuclei and longitudinal cell growth, do not necessarily indicate sufficient dystrophin expression. Seeding MyoD-positive cells at high density ($>5.0\times10^4$ cells/cm^2) and incubating for longer periods (>2 weeks) were critical to induce sufficient dystrophin expression. Detachment of differentiated myotubes from culture wells was also problematic; supporting them with a coating matrix seems to promise better results.

Direct translation of antisense PMO from dog to human was feasible

We previously reported systemic multi-exon skipping in CXMD$_J$ with a 3-antisense PMO cocktail and amelioration of dystrophic pathology [6]. The effectiveness of the 3-antisense PMO cocktail was confirmed in MyoD-transduced fibroblasts derived from DMD 8772 as well. When the dog and human sequences were compared, 97% of dystrophin exon 6 and 95% of dystrophin exon 8 matched on the sequence level. This similarity enabled use of the unified antisense design methodology targeting the same sequence. We demonstrated that the identical antisense PMO sequence designed for dog and achieved multi-skipping of exons 6 and 8 in human cells. The skipping efficacies of the PMOs were indistinguishable between CXMD$_J$ and DMD 8772; the superior efficacy of the four-PMO cocktail against that of the three-PMO cocktail and the equivalent efficacies of each four-PMO cocktail were comparable. CXMD$_J$ shows more similarity in the pathogenic phenotype to human DMD than to *mdx* mice [24]. These findings imply that not only the similarity in the sequence but also the similarity in the pathogenic phenotype contributed to the comparable results.

No study has yet compared the exon skipping due to identical antisense PMOs between cells of different species carrying same exon deletion in mRNA. Recent investigations have reported a limitation in designing efficient antisenses to induce human dystrophin skipping in a mice model assay [25]; however, we confirmed the feasibility of direct translation of an antisense PMO from a DMD dog model to a DMD patient, at least *in vitro*, for the first time.

The four-antisense PMO cocktail, the addition of a fourth antisense sequence to the three-antisense PMO cocktail, increased the efficiency of skipping as previously reported [26,27]. The effectiveness of the four-antisense PMO cocktails, however, must be evaluated *in vivo*, and we are planning systemic treatment of $CXMD_J$ with them. Our results underscore the usefulness of $CXMD_J$ as a DMD model for translational research and advance the prospect that systemic treatment of the DMD patient by multi-exon skipping is possible.

Mode of exon 9 skipping might be affected by frequency of alternative splicing

With the antisense PMO targeting exons 6 and 8, exon 9 was always skipped in $CXMD_J$, although it was only partially skipped in DMD 8772. Two possibilities were considered to explain the difference: (1) the effects of the shortened introns 6 and 7 due to the deletion around exon 7 in DMD 8772 (**Figure 5**), and (2) the different frequencies of alternative splicing of exon 9. For the former case, we tried exon 8 skipping using a combination of Ex8A and Ex8G in normal and affected human MyoD-transduced fibroblasts, and found that the skipping of exon 8 and exons 8/9 happened simultaneously (**Figure S1**). Therefore, it is unlikely that the intron length affects the difference. In the latter case, the untreated MyoD-transduced fibroblasts from $CXMD_J$ clearly showed one normal and one alternative transcript; on the other hand, the untreated sample from DMD 8772 showed only a normal transcript, suggesting that the frequency of alternative splicing of exon 9 is an underlying factor in the difference. It was reported that an antisense oligonucleotide targeting exon 8 facilitates the skipping of exon 9 as well as exon 8 by effecting the concatenation of exons 8 and 9 in human and dog cells [28].

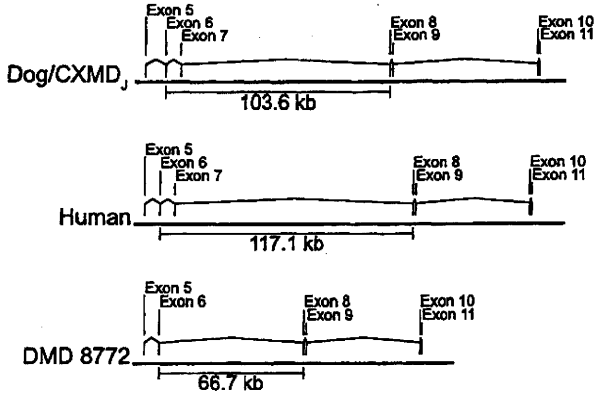

Figure 5. Location of dystrophin exons 5 to 11 in the genome. Distances from dystrophin exon 6 to exon 8 are indicated based on the GenBank reference sequences of *Canis familiaris* chromosome X genomic contig, whole genome shotgun sequence (NW_879562.1) and *Homo sapiens* 211000035840903 genomic scaffold, whole genome shotgun sequence (CH471074.1).
doi:10.1371/journal.pone.0012239.g005

These findings were observed in myoblasts but not in MyoD-tansduced fibroblasts [29,30,31]. As is well known, the mode of alternative splicing differs among various tissues [32,33], and our MyoD-transduced fibroblasts might have characteristics that are incompatible with the alternative splicing of exon 9.

In summary, MyoD transduction of fibroblasts with the help of FACS may be practical for exon skipping assays, and the direct translation of an antisense PMO from a DMD dog model to a DMD patient was feasible *in vitro*, suggesting that the animal model-based antisense PMO for multiple skipping could be effective for humans as well.

Materials and Methods

Ethics Statement

The patient samples were collected and used with the approval of the Ethics Committee of the National Center of Neurology and Psychiatry, approval ID: 20-4-6. Written informed consent was obtained from the donor. The dog study was approved by the Ethics Committee for the Treatment of Middle-sized Laboratory Animals of the National Center of Neurology and Psychiatry, approval ID: 20-05.

Cell culture

Dog primary myoblasts and fibroblasts were obtained from muscle specimens of normal and affected neonatal dogs of the $CXMD_J$ colony using a standard pre-plating technique. Primary fibroblasts of the DMD patient (DMD 8772) were obtained from skin explants and peripheral blood lymphocytes using Lymphocyte Separating Medium (PAN Biotech GmbH, Aidenbach, Germany). Lymphoblastoid cell lines were established by transformation with Epstein-Barr virus. The normal human fibroblast cell line TIG-119 was obtained from the Health Science Research Resource Bank (Osaka, Japan). Fibroblasts were cultured in 20% or 10% growth medium containing DMEM/F-12 1:1 (Invitrogen, San Diego, CA, USA), 20% or 10% fetal bovine serum, and 1% penicillin/streptomycin. For differentiation to myotubes, FACS-sorted MyoD-transduced fibroblasts were cultured in 2% differentiation medium containing DMEM/F-12 1:1, 2% horse serum, ITS Liquid Media Supplement (Sigma-Aldrich, St. Louis, MO, USA), and 1% penicillin/streptomycin.

Genomic mutation analysis

The dystrophin exon 7-deletion of DMD 8772 had been identified previously by MLPA. For breakpoint detection, lymphocyte genomic DNA was used as a template. Seven pairs of intron-spanning primers, positioned in the intron 6/7, were designed to yield 150-600 bp PCR products. A failure of PCR indicated deletions spanning the primer annealing sites. Four of seven primer pairs showed no amplification, suggesting that the deletion was more than 3.5 kb and less than 64.4 kb. Additionally, two intron 6 sense-primers and eight intron 7 antisense-primers were designed. Each primer pair was placed by flanking the breakpoint and expected to yield PCR products within the range of 4–64 kb. Primer sequences are available on request. PCR was performed using Phusion Hot Start High-Fidelity DNA Polymerase (Finnzymes, Keilaranta, Finland), and the cycling program was set to yield 16 kb products with a program of 35 cycles of 98°C for 10 sec, 60°C for 30 sec, and 72°C for 450 sec. Failure of PCR indicated products of more than 16 kb in size or the deletion of annealing sites. The breakpoint region was thus narrowed down to 2.5 kb, then primer walk sequencing was performed (Operon Biotechnologies, Tokyo, Japan).

MyoD transduction and cell sorting by FACS

The coding sequences of mouse *Myod1* (CCDS 21277.1) and human *MYOD1* (CCDS 7826.1) were derived from the Consensus CDS database [34]. The sequences were synthesized and cloned into a pUC57 vector (GenScript, Piscataway, NJ, USA). We subcloned it into a pRetroX-IRES-ZsGreen1 expression vector (Clontech, Mountain View, CA, USA). The expression vector, a pVSV-G envelope vector, and a gap-pol expression vector were co-transfected into a 293T packaging cell line using the standard calcium phosphate method. After 48–72 h incubation, the viral supernatant was collected and stored at −80°C. For retroviral transduction, the fibroblasts were harvested at 70–80% confluence in a T225 flask, and 2.5 ml thawed retroviral stock was added to 35 ml of growth medium. We added polybrene (Sigma-Aldrich) to a final concentration of 8 μg/ml. After 48–72 h incubation at 32°C, the culture medium was replaced with fresh growth medium, the cells were incubated at 37°C 1–3 d more, until the GFP-positive cells exceeded approximately 60%. Cell sorting was performed on a FACS VantageSE or FACSAria flow cytometry system (BD Bioscience, Franklin Lakes, NJ, USA). The recovered GFP-positive cells were seeded in Matrigel (BD Bioscience)-coated well plates at density of 5×10^4 cell/cm^2. After confirmation of cell attachment, the culture medium was changed to 2% differentiation medium. We cultured MyoD-transduced fibroblasts for 10 to 16 d to differentiate to myotubes.

Antisense PMO design and transfection to cultured cells

The antisense PMO sequences Ex6A, Ex6B, and Ex8A were described in Yokota et al. [6]. In addition, extra sequences hEx6B, Ex8G, Ex8I, and Ex8K were designed and synthesized (Gene Tools, LLC, Philomath, OR, USA). We used the Human Splicing Finder for *in silico* prediction of the splice-enhancer motifs [35]. All sequences are shown in **Table S1**. We transfected the antisense PMOs into myotubes differentiated from MyoD-transduced fibroblasts with a transfection agent, Endo-Porter (Gene Tools). In the 2% differentiation medium, the final concentration of the antisense PMO was 10 μM for a single sequence, 20 μM for two sequences, and a total of 30 μM for three or four sequences. A final concentration of Endo-Porter was 6 μM. After 48–72 h incubation with the PMO, the medium was changed to a fresh culture medium free of PMOs. The cells were recovered for analysis after 24–48 h in the PMO-deprived medium to allow sufficient time to translate dystrophin protein.

Quantitative RT-PCR analysis

Total RNA was extracted from MyoD-transduced fibroblasts obtained from normal subjects using Trizol (Invitrogen) at the time points specified. Total RNA (100-200 ng) was employed for cDNA synthesis using a QuantiTect Reverse Transcription Kit (Qiagen, Hilden, Germany). Quantitative real-time PCR was performed using ExTaq II SYBR (Takara, Kyoto, Japan) and a MyiQ Single-Color Real-Time PCR detection system (Bio-Rad, Hercules, CA). Primer sequences are shown in **Table S2**. Expression of dystrophin mRNA was normalized to *GAPDH* mRNA, and the time course of the increment was calculated by the delta-delta-Ct method.

RT-PCR and sequence analysis

As well as quantitative RT-PCR analysis, total RNA extraction and cDNA synthesis were performed. For myoblasts and MyoD-transduced fibroblasts, 35 cycles of denaturing at 98°C for 10 sec, annealing at 63°C for 30 sec, and extension at 72°C for 1 min were performed with ExTaq DNA polymerase (Takara). For fibroblasts and lymphoblasts, nested PCR was performed. Primer sequences are shown in **Table S3**. PCR products were electrophoresed on 1.2% SeaKem LE agarose gel (Lonza, Basel, Switzerland). The bands of interests were excised using a Wizard SV Gel and PCR Clean-Up system (Promega, Fitchburg, WI, USA), then sequenced directly or cloned into a vector using a TOPO-TA Cloning Kit (Invitrogen) with standard cloning techniques. Sequencing was performed by Fasmac Corporation (Kanagawa, Japan).

Immunostaining analysis

Cells were fixed in 3% paraformaldehyde, permeabilized in 10% Triton-X, then blocked by 10% goat serum in PBS for 1 h at room temperature. The cells were incubated with the primary antibody for 1 h at room temperature using anti-dystrophin (NCL-Dys1, diluted 1:30, Novocastra, Newcastle upon Tyne, UK), anti-myosin heavy chain (NCL-MHCf, diluted 1:30, Novocastra), anti-MyoD (NCL-MyoD1, diluted 1:30, Novocastra), or anti-desmin (NCL-DES-DERII, diluted 1:30, Novocastra). Incubation with the secondary antibody was performed for 30 min at room temperature using anti-rabbit or anti-mouse IgG (Alexa Fluor 546 highly cross-adsorbed, diluted 1:300, Invitrogen). Antibodies were diluted in Can Get Signal Immunostain A solution (Toyobo, Osaka, Japan). To visualize nuclei and enhance fluorescence signals, cells were mounted with Pro Long Gold Antifade reagent (Invitrogen).

Immunoblotting analysis

Protein was extracted from cultured cells using RIPA buffer (Thermo Fisher Scientific, Rockford, IL, USA) containing Complete Mini (Roche Applied Science, Indianapolis, IN, USA) as a protease inhibitor. Protein concentrations were determined using a BCA protein assay kit (Thermo Fisher Scientific) and equalized. After being mixed with an equal volume of EzApply sample buffer (ATTO Corporation, Tokyo, Japan), cell lysates containing equal amounts of total protein were denatured at 95°C for 5 min, electrophoresed in NuPAGE Novex Tris-Acetate Gel 3–8% (Invitrogen) at 150 V for 75 min, and transferred onto an Immobilon-P membrane (Millipore Corp., Billerica, MA, USA). Membranes were blocked for 1 h with 5% ECL Blocking agent (GE Healthcare, Buckinghamshire, UK) and probed with anti-dystrophin antibody (NCL-Dys1, diluted 1:50, Novocastra), followed by incubation with peroxidase-conjugated goat-anti-mouse IgG (Bio-Rad). An ECL Plus Western blotting system (GE Healthcare) was used to detect protein bands.

Supporting Information

Figure S1 RT-PCR of dystrophin mRNA isolated from the normal and affected human MyoD-transduced fibroblasts after the single exon 8 skipping.
Found at: doi:10.1371/journal.pone.0012239.s001 (0.30 MB PDF)

Table S1 Sequences of antisense PMO for dystrophin gene (for dog and human if not specified).
Found at: doi:10.1371/journal.pone.0012239.s002 (0.07 MB PDF)

Table S2 Sequences of qRT-PCR primers.
Found at: doi:10.1371/journal.pone.0012239.s003 (0.07 MB PDF)

Table S3 Sequences of RT-PCR primers.
Found at: doi:10.1371/journal.pone.0012239.s004 (0.07 MB PDF)

Acknowledgments

The authors thank Yu-ichi Goto (Department of Mental Retardation and Birth Defect Research, National Center of Neurology and Psychiatry), Narihiro Minami (Department of Neuromuscular Research, National Center of Neurology and Psychiatry), Hirofumi Komaki (Department of Child Neurology, National Center of Neurology and Psychiatry), Katsutoshi Yuasa (Research Institute of Pharmaceutical Sciences, Faculty of Pharmacy, Musashino University, Tokyo, Japan), and Tetsuya Nagata, Yuko Shimizu, and Satoru Masuda (Department of Molecular Therapy, National Center of Neurology and Psychiatry) for useful discussions and technical assistance.

Author Contributions

Conceived and designed the experiments: TS AN ST. Performed the experiments: TS YA. Analyzed the data: TS MO. Contributed reagents/materials/analysis tools: TY TO. Wrote the paper: TS AN ST.

References

1. Aartsma-Rus A, Bremmer-Bout M, Janson AA, den Dunnen JT, van Ommen GJ, et al. (2002) Targeted exon skipping as a potential gene correction therapy for Duchenne muscular dystrophy. Neuromuscul Disord 12(Suppl 1): S71–77.
2. Mann C, Honeyman K, Cheng A, Ly T, Lloyd F, et al. (2001) Antisense-induced exon skipping and synthesis of dystrophin in the mdx mouse. Proc Natl Acad Sci U S A 98: 42–47.
3. Alter J, Lou F, Rabinowitz A, Yin H, Rosenfeld J, et al. (2006) Systemic delivery of morpholino oligonucleotide restores dystrophin expression bodywide and improves dystrophic pathology. Nat Med 12: 175–177.
4. van Deutekom J, Janson A, Ginjaar I, Frankhuizen W, Aartsma-Rus A, et al. (2007) Local dystrophin restoration with antisense oligonucleotide PRO051. N Engl J Med 357: 2677–2686.
5. Kinali M, Arechavala-Gomeza V, Feng L, Cirak S, Hunt D, et al. (2009) Local restoration of dystrophin expression with the morpholino oligomer AVI-4658 in Duchenne muscular dystrophy: a single-blind, placebo-controlled, dose-escalation, proof-of-concept study. Lancet Neurol 8: 918–928.
6. Yokota T, Lu Q, Partridge T, Kobayashi M, Nakamura A, et al. (2009) Efficacy of systemic morpholino exon-skipping in Duchenne dystrophy dogs. Ann Neurol 65: 667–676.
7. Sharp N, Kornegay J, Van Camp S, Herbstreith M, Secore S, et al. (1992) An error in dystrophin mRNA processing in golden retriever muscular dystrophy, an animal homologue of Duchenne muscular dystrophy. Genomics 13: 115–121.
8. Béroud C, Tuffery-Giraud S, Matsuo M, Hamroun D, Humbertclaude V, et al. (2007) Multiexon skipping leading to an artificial DMD protein lacking amino acids from exons 45 through 55 could rescue up to 63% of patients with Duchenne muscular dystrophy. Hum Mutat 28: 196–202.
9. Wee K, Pramono Z, Wang J, MacDorman K, Lai P, et al. (2008) Dynamics of co-transcriptional pre-mRNA folding influences the induction of dystrophin exon skipping by antisense oligonucleotides. PLoS ONE 3: e1844.
10. Pramono Z, Takeshima Y, Alimsardjono H, Ishii A, Takeda S, et al. (1996) Induction of exon skipping of the dystrophin transcript in lymphoblastoid cells by transfecting an antisense oligodeoxynucleotide complementary to an exon recognition sequence. Biochem Biophys Res Commun 226: 445–449.
11. Chelly J, Gilgenkrantz H, Hugnot J, Hamard G, Lambert M, et al. (1991) Illegitimate transcription. Application to the analysis of truncated transcripts of the dystrophin gene in nonmuscle cultured cells from Duchenne and Becker patients. J Clin Invest 88: 1161–1166.
12. Aartsma-Rus A, Janson A, Kaman W, Bremmer-Bout M, den Dunnen J, et al. (2003) Therapeutic antisense-induced exon skipping in cultured muscle cells from six different DMD patients. Hum Mol Genet 12: 907–914.
13. Aartsma-Rus A, Janson A, Kaman W, Bremmer-Bout M, van Ommen G, et al. (2004) Antisense-induced multiexon skipping for Duchenne muscular dystrophy makes more sense. Am J Hum Genet 74: 83–92.
14. Gonçalves M, Swildens J, Holkers M, Narain A, van Nierop G, et al. (2008) Genetic complementation of human muscle cells via directed stem cell fusion. Mol Ther 16: 741–748.
15. Cooper S, Kizana E, Yates J, Lo H, Yang N, et al. (2007) Dystrophinopathy carrier determination and detection of protein deficiencies in muscular dystrophy using lentiviral MyoD-forced myogenesis. Neuromuscul Disord 17: 276–284.
16. Zheng J, Wang Y, Karandikar A, Wang Q, Gai H, et al. (2006) Skeletal myogenesis by human embryonic stem cells. Cell Res 16: 713–722.
17. McClorey G, Moulton H, Iversen P, Fletcher S, Wilton S (2006) Antisense oligonucleotide-induced exon skipping restores dystrophin expression in vitro in a canine model of DMD. Gene Ther 13: 1373–1381.
18. Reiss J, Rininsland F (1994) An explanation for the constitutive exon 9 cassette splicing of the DMD gene. Hum Mol Genet 3: 295–298.
19. Miller A, Buttimore C (1986) Redesign of retrovirus packaging cell lines to avoid recombination leading to helper virus production. Mol Cell Biol 6: 2895–2902.
20. Morgenstern J, Land H (1990) A series of mammalian expression vectors and characterisation of their expression of a reporter gene in stably and transiently transfected cells. Nucleic Acids Res 18: 1068.
21. Choi J, Costa M, Mermelstein C, Chagas C, Holtzer S, et al. (1990) MyoD converts primary dermal fibroblasts, chondroblasts, smooth muscle, and retinal pigmented epithelial cells into striated mononucleated myoblasts and multinucleated myotubes. Proc Natl Acad Sci U S A 87: 7988–7992.
22. Etzion S, Barbash I, Feinberg M, Zarin P, Miller L, et al. (2002) Cellular cardiomyoplasty of cardiac fibroblasts by adenoviral delivery of MyoD ex vivo: an unlimited source of cells for myocardial repair. Circulation 106: I125–130.
23. Noda T, Fujino T, Mie M, Kobatake E (2009) Transduction of MyoD protein into myoblasts induces myogenic differentiation without addition of protein transduction domain. Biochem Biophys Res Commun 382: 473–477.
24. Shimatsu Y, Yoshimura M, Yuasa K, Urasawa N, Tomohiro M, et al. (2005) Major clinical and histopathological characteristics of canine X-linked muscular dystrophy in Japan, CXMDJ. Acta Myol 24: 145–154.
25. Mitrpant C, Adams A, Meloni P, Muntoni F, Fletcher S, et al. (2009) Rational design of antisense oligomers to induce dystrophin exon skipping. Mol Ther 17: 1418–1426.
26. Aartsma-Rus A, Kaman W, Weij R, den Dunnen J, van Ommen G, et al. (2006) Exploring the frontiers of therapeutic exon skipping for Duchenne muscular dystrophy by double targeting within one or multiple exons. Mol Ther 14: 401–407.
27. Harding P, Fall A, Honeyman K, Fletcher S, Wilton S (2007) The influence of antisense oligonucleotide length on dystrophin exon skipping. Mol Ther 15: 157–166.
28. Aartsma-Rus A, van Ommen G (2007) Antisense-mediated exon skipping: a versatile tool with therapeutic and research applications. RNA 13: 1609–1624.
29. Wilton S, Fall A, Harding P, McClorey G, Coleman C, et al. (2007) Antisense oligonucleotide-induced exon skipping across the human dystrophin gene transcript. Mol Ther 15: 1288–1296.
30. McClorey G, Fall A, Moulton H, Iversen P, Rasko J, et al. (2006) Induced dystrophin exon skipping in human muscle explants. Neuromuscul Disord 16: 583–590.
31. Aartsma-Rus A, De Winter C, Janson A, Kaman W, Van Ommen G, et al. (2005) Functional analysis of 114 exon-internal AONs for targeted DMD exon skipping: indication for steric hindrance of SR protein binding sites. Oligonucleotides 15: 284–297.
32. Hallegger M, Llorian M, Smith C (2010) Alternative splicing: global insights. FEBS J 277: 856–866.
33. Sironi M, Cagliani R, Pozzoli U, Bardoni A, Comi G, et al. (2002) The dystrophin gene is alternatively spliced throughout its coding sequence. FEBS Lett 517: 163–166.
34. Pruitt K, Harrow J, Harte R, Wallin C, Diekhans M, et al. (2009) The consensus coding sequence (CCDS) project: Identifying a common protein-coding gene set for the human and mouse genomes. Genome Res 19: 1316–1323.
35. Desmet F, Hamroun D, Lalande M, Collod-Béroud G, Claustres M, et al. (2009) Human Splicing Finder: an online bioinformatics tool to predict splicing signals. Nucleic Acids Res 37: e67.

筋ジストロフィーの新しい治療戦略*

武田　伸一**

Key Words : Duchenne muscular dystrophy, dystrophin, exon skipping, dystrophic dog, mdx 52 mice

はじめに

筋ジストロフィーは「骨格筋の変性，壊死を主病変とし，臨床的には進行性の筋力低下をみる遺伝性の疾患である」と定義される．筋ジストロフィーの原因遺伝子の多くは筋細胞膜のタンパク質，中でもジストロフィン・糖タンパク質複合体（dystrophin-glycoprotein complex : DGC）の構成分子をコードしており，この複合体が骨格筋膜の安定性に重要である事を示唆する．デュシェンヌ型筋ジストロフィー（Duchenne muscular dystrophy : DMD）はDMD遺伝子の変異によりDGCの中心分子であるジストロフィンが欠損することで発症し，ジストロフィンの欠損が不完全な場合はベッカー型筋ジストロフィー（Becker type progressive muscular dystrophy : BMD）の表現型を呈する．DMDは，X染色体連鎖性遺伝形式をとり，筋ジストロフィーの中で最も頻度が高く，新生男児3,500人に1人の割合で発症する．DMD患者は2～5歳時に歩行異常で気付かれることが多く，進行性の筋力低下のため11～13歳前後に独立歩行が不可能になり，以後呼吸不全や心不全で死亡に至る．最近，呼吸管理の進歩により，約10年間寿命が延長しているが，有効と認められている治療は副腎皮質ステロイドと脊椎変形に対する手術，呼吸補助と心不全に対する薬物療法のみであり，未だ筋変性・壊死を阻止する決定的な治療法はない．そこで，先進的な治療である遺伝子治療，幹細胞移植治療を含めて，治療法の開発研究が世界各国で，極めて活発に進められている．

I．Anti-sense oligonucleotides（AOs）によるエクソン・スキップ

人工的に合成された短い核酸化合物であるAOsを用いて行われるエクソン・スキップ誘導療法では，pre mRNAからmRNAへのスプライシング過程で，遺伝子変異を持つ，あるいはその近傍のエクソンを人為的にスキップさせて，アウト・オブ・フレーム変異をイン・フレーム変異に変換することを企図する．誘導されるジストロフィンは，正常なジストロフィンのタンパク質構造を一部欠くことになるが，actin結合ドメインやcysteine-richドメイン，C端ドメインなどの重要な分子構造は保存される．

* New Therapeutic Strategies to Duchenne Muscular Dystrophy.

** 独立行政法人国立精神・神経医療研究センタートランスレーショナル・メディカルセンター・神経研究所遺伝子疾患治療研究部
Shin'ichi Takeda : Translational Medical Center, National Center of Neurology and Psychiatry. Department of Molecular Therapy, National Institute of Neuroscience, National Center of Neurology and Psychiatry

現在，筋ジストロフィーのモデル動物を用いたin vitroおよびin vivoでの研究や臨床治験に使用されている代表的なAOsには，2'-O-methyl phosphorothioate antisense oligoribonucleotide (2OMeAO)，phosphorodiamidate morpholino oligomer（PMOあるいはモルフォリノ）がある．特に，PMOは，ヌクレアーゼなど生体内の酵素による分解を受けずに，免疫応答を誘導しないPMO環構造を持つ水溶性の核酸類似人工化合物である[1,2]．しかも，塩基間の分子距離を維持するように設計されており，標的pre mRNAに対し非常に強い配列特異的結合を可能にしている一方，電荷を持たないため，細胞膜の通過性が低い点が課題として指摘されていた．

最近，国立精神・神経医療研究センターでコロニーを確立したDMDのモデル動物である筋ジストロフィー犬，CXMDJ[3]に対してPMOの筋肉内局所および全身投与が行われた[4]．筋ジストロフィー犬は，ジストロフィン遺伝子のイントロン6のスプライス・サイトに点変異を持ち，エクソン7をスキップしてエクソン8にストップ・コドンを生ずるため，ジストロフィンを発現していない．そこで，アミノ酸の読み枠を修正するためにエクソン6および8を標的とした合計3種類のAOsをカクテルにして投与を行った結果，心筋を除く全身骨格筋においてジストロフィンの発現が回復し，血清CK値も軽減し，病理組織学所見も改善した．また，PMO非投与の筋ジストロフィー犬と比較し，投与筋ジストロフィー犬では骨格筋のMRIで，筋の変性や壊死の改善が示唆され，運動機能をはじめとする臨床症状の改善も認められた．一方で，血液検査や諸臓器の病理組織学上，副作用の徴候は全く認められず，PMOおよび発現誘導されたジストロフィンに対する免疫反応は観察されなかった[4]．本研究により，複数のエクソンを同時にスキップすることが可能になったことから，エクソン・スキップの対象となるDMD患者の範囲が拡大し，遺伝子欠失によるDMDの約80%に達したことが特筆される．

エクソン6/8スキップ療法の限界の一つとしては，対象となる遺伝子変異を持つDMD患者の数が極めて限られていることが挙げられていた．ところが，DMD遺伝子エクソン7欠失を有するDMD患者が国内で見出された．患者本人及び家族の同意の下，国立精神・神経医療研究センター病院に入院して頂き，皮膚生検を実施することができた．生検材料から，線維芽細胞株を擁立し，MyoD遺伝子を導入して筋芽細胞に転換した上で，筋ジストロフィー犬で得られた配列を下に，PMOによるエクソン・スキップを試み，RT-PCR上でのエクソン6/8スキップと，免疫染色とWestern blotによるジストロフィンの発現を確認することができた．本研究により，モデル動物のみでなくDMD患者に於いてDMD遺伝子のエクソン6と8のスキップ療法を行う根拠が得られたものと考えている[5]．

II．エクソン・スキッピング治療の今後の見通しと問題点

DMD遺伝子のエクソン6/8スキップに関しては，前臨床試験を進め，DMD患者由来の細胞を用いたin vitro試験でも良好な結果が得られたとは言え，対象となる患者数に制限があることには疑いがない．そこでDMDで見出される変異が集中しているエクソン45から55の領域（所謂ホットスポット領域）に注目して検索したところ，エクソン51のスキップに成功すれば，遺伝子欠失によるDMD患者の約15%について，イン・フレーム化できることが明らかになった．しかし，それを実証するためには，疾患モデル動物を用いた検証が必要である．そこで，以前に我々からの要請に基づいて開発されたDMD遺伝子のエクソン52を欠いた筋ジストロフィーマウス（mdx52マウス）[6]を用いてエクソン51スキップが可能であって表現型を改善する効果があるかどうか検証した．最初にmdx52マウス前脛骨筋にPMOを筋注することによりエクソン51スキップが可能なアンチセンス配列の組み合わせを検証した．その上で，最適な組み合わせのPMOについて尾静脈経由の全身投与実験を行った．その結果，エクソン51スキップにより，心筋を除く全身の骨格筋でジストロフィンの発現が回復し血清CK値，筋張力，組織像をはじめとする表現型の改善が認められた．少なくともmdx52マウスにおいては，エクソン51スキップの有効性が検証されたと言える[7]．

現在，DMD患者に対する臨床治験として，オ

ランダやイギリスで，エクソン51を標的とした2OMeAOやPMOの全身投与が進められている．2OMeAOを用いた治験に関しては，6mg/kgの投与量で，皮下注による全身投与が行われ，比較的少数のDMD患児に対する24週までの投与では，6分間歩行試験において良好な臨床的な効果が得られている．一方で，蛋白尿等の懸念も指摘されている．PMOを用いた治験に関しては，比較的少数のDMD患児を対象に12週までの投与が行われた結果，投与量に応じてジストロフィンの発現が認められ，何ら毒性は観察されなかった．しかし，20mg/kgまでの投与の範囲では，臨床的な有効性が観察されなかったことが指摘されている．

ただし，これまでの研究結果からエクソン・スキッピング治療を臨床応用するために解決しなければならない問題点も明らかとなった．

1つのエクソンを標的としたシングル・エクソン・スキップは，治療対象となる患者数に限りがあり，しかもそれぞれの遺伝子変異に応じたAOsが必要となる（テーラーメイド治療）．そのため複数のAOsを混合して広範囲のエクソンをスキップさせるマルチ・エクソン・スキッピング療法が期待されている．この手法は，シングル・エクソン・スキップ療法よりも比較的多くのDMD患者をカバーすることができる．例えば，エクソン45-55の欠損患者のうち94%が軽症のBMDと報告されていることから，DMDのホットスポット変異として知られているエクソン45-55の範囲内に大小の欠失を持つDMD患者に対してエクソン45-55をまとめてスキップする共通した治療が可能となる．

一方，これまで検討されてきた2OMeAOやPMOでは，心筋での効率は低いことが指摘されている．近年，ペプチドの血清中や細胞内での安定性の増加，物質のエンドソームでのトラップの減少および核酸の細胞内への取り込みを増加させる目的で，PMOに細胞膜透過性ペプチド（CPPs）であるアルギニン，6-アミノヘキサン酸，および/またはβ-アラニンを付加したpeptide-linked PMO（PPMO）が開発された[8]．

III．結論

ジストロフィン欠損によるDMD患者に関しては呼吸不全，心不全対策の発展に伴い寿命が延長しているものの，疾患の本態に根ざした治療はいまだ確立されておらず，治療法の開発が急務である．近年，欧米ではDMD患者に対する臨床治験が開始され，その動きが日本にも及ぼうとしている．DMDに対する治療研究で開発された技術，特にPMOあるいは，筋ジストロフィーの他の病型のみならず，多くの遺伝性神経・筋疾患にも応用が期待される．

文　献

1）Nakamura A, Takeda S : Exon-skipping therapy for Duchenne muscular dystrophy. Neuropathology 29 : 494-501, 2009

2）Miyagoe-Suzuki Y, Takeda S : Gene therapy for muscle disease. Exp Cell Res 316 : 3087-3092, 2010

3）Urasawa N, Wada MR, Machida N et al : Selective vacuolar degeneration in dystrophin deficient canine Purkinje fibers despite preservation of dystrophin-associated proteins with overexpression of Dp71. Circulation 117 : 2437-2448, 2008

4）Yokota T, Lu QL, Partridge T et al : Efficacy of systemic morpholino exon-skipping in duchenne dystrophy dogs. Ann Neurol 65 : 667-676, 2009

5）Saito T, Nakamura A, Aoki Y et al : Antisense PMO Found in Dystrophic Dog Model Was Effective in Cells from Exon 7-Deleted DMD Patient. PLoS One 5 (8) : e12239, 2010

6）Araki E, Nakamura K, Nakao K et al : Targeted disruption of exon 52 in the mouse dystrophin gene induced muscle degeneration similar to that observed in Duchenne muscular dystrophy. Biochem Biophys Res Commun 238 : 492-497, 1997

7）Aoki Y, Nakamura A, Yokota T et al : In-frame dystrophin following exon 51-skipping improves muscle pathology and function in the exon 52-deficient mdx mouse. Mol Ther 18 : 1995-2005, 2010

8）Yokota T, Lu QL, Partridge TA et al : A renaissance for antisense oligonucleotide drugs in neurology : exon skipping breaks new ground. Arch Neurol 66 : 32-38, 2009

New Therapentic Strategies to Duchenne Muscular Dystrophy

Shin'ichi TAKEDA

Translational Medical Center, National Center of Neurology and Psychiatry
Department of Molecular Therapy, National Institute of Neuroscience,
National Center of Neurology and Psychiatry

Duchenne muscular dystrophy (DMD) is a lethal muscle disorder caused by the mutations of the DMD gene, which encodes a 427-kDa spectrin-like cytoskeletal protein, dystrophin. Exon skipping by antisense oligonucleotides is a novel method to restore the reading frame of the mutated DMD gene, and rescue dystrophin expression. We recently demonstrated that systemic delivery of Morpholino antisense oligonucleotides targeting exon 6 and 8 of the canine DMD gene, efficiently recovered functional dystrophin at the sarcolamma of dystrophic dogs, and improved performance of affected dogs without serious side effects (Yokota et al., Ann Neurol, 2009). We, then, experienced an exon 7-deleted DMD patient in Japan and got cultured fibroblasts from biopsy specimen. We converted these cells into myogenic cells by MyoD cDNA transfection and examined skipping efficiency of exon 6 and 8 of the DMD gene. We observed effective skipping of these exons and recovery of dystrophin expression on the cells (Saito et al., PLoS One, 2010) We also optimized antisense Morpholinos targeting exon 51 of the mouse DMD gene, to prepare clinical trials for the DMD patients with frequent mutations of the DMD gene. A combination of two Morpholinos showed an excellent restoration of sarcolemmal dystrophin in injected muscle or after systemic delivery, and amelioration of dystrophic pathology, and improvement of contractile force (Aoki et al., Mol Ther, 2010). Clinical trials of exon 51 skipping are under way in DMD patients at this moment.

CHAPTER NINE

Multifunctional Roles of Activins in the Brain

Hiroshi Ageta *and* Kunihiro Tsuchida

Contents

I. Introduction 186
II. Expression Pattern of Activin and Activin Receptor in the Brain 187
III. Activin Receptor and its Regulatory Proteins 188
IV. Functions of Activins in the CNS 189
A. Activin regulates spine formation 189
B. Activin influences depression and anxiety-related behavior 190
C. Activin is an important factor in adult neurogenesis 193
D. Activin is a key player for maintaining late-phase LTP 195
E. Activin influences reconsolidation and extinction 196
V. Conclusion and Perspectives 200
Acknowledgments 201
References 201

Abstract

Activins, which are members of the TGF-β superfamily, were initially isolated from gonads and served as modulators of follicle-stimulating hormone secretion. Activins regulate various biological functions, including induction of the dorsal mesoderm, craniofacial development, and differentiation of numerous cell types. Activin receptors are highly expressed in neuronal cells, and activin mRNA expression is upregulated by neuronal activity. Activins also exhibit neuroprotective action during excitotoxic brain injury. However, very little is known about the functional roles of activins in the brain. We recently generated various types of transgenic mice, demonstrating that activins regulate spine formation, behavioral activity, anxiety, adult neurogenesis, late-phase long-term potentiation, and maintenance of long-term memory. The present chapter describes recent progress in the study of the role of activin in the brain.

Division for Therapies against Intractable Diseases, Institute for Comprehensive Medical Science (ICMS), Fujita Health University, Toyoake, Aichi, Japan

Vitamins and Hormones, Volume 85
ISSN 0083-6729, DOI: 10.1016/B978-0-12-385961-7.00009-3

I. Introduction

In 1986, during inhibin purification, activin, a regulating factor for secretion of follicle-stimulating hormone from pituitary cells was discovered (Ling *et al.*, 1986; Vale *et al.*, 1986). For more than 20 years after its discovery, numerous studies have shown that activins serve as multifunctional growth and differentiation factors in many cell types (Mather *et al.*, 1997; Ying *et al.*, 1997).

Activins are dimeric glycoproteins, which are formed by two of four different β subunits of inhibin in mammals (βA, βB, βC, and βE; Tsuchida, 2004). βA and βB transcripts exist in almost all tissues. In contrast, βC and βE subunits are predominantly expressed in the liver. Homodimers of inhibin βA or βB subunits, activin A and activin B, respectively, exist in various tissues (Nakamura *et al.*, 1992), and heterodimeric activin AB has also been isolated from porcine follicular fluid (Ling *et al.*, 1986; Nakamura *et al.*, 1992).

Activins directly bind to serine/threonine kinase activin type II receptors (ActRII and ActRIIB), which are located on the cell membrane (Pangas and Woodruff, 2000; Fig. 9.1). Once the ligand is bound, type II receptors

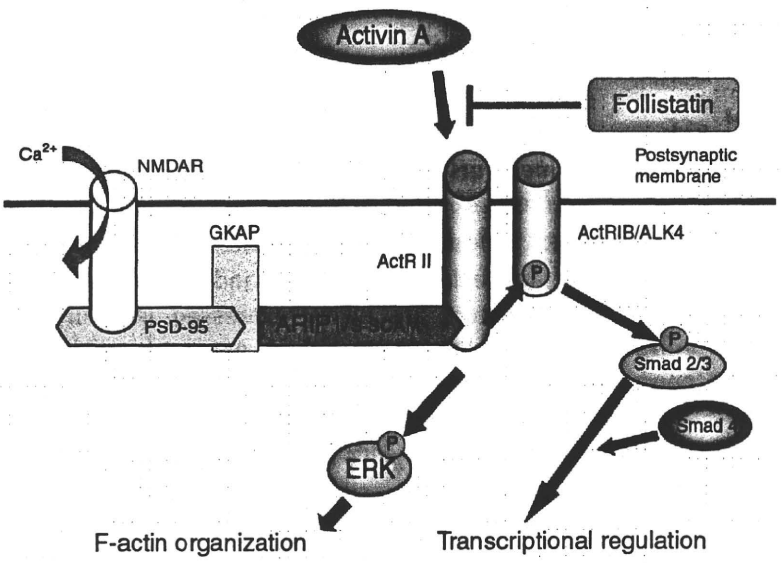

Figure 9.1 Activin-signaling cascade in the postsynaptic region. Activin A binds directly to activin type II receptor (ActRII or ActRIIB). Following binding, ActRIIs phosphorylate activin type I receptors (ActRIB or ALK4). ActRIB phosphorylates the transcriptional factor Smad2/3, and phosphorylated Smad2/3 binds to Smad4. Smad complexes translocate to the nucleus and regulate transcriptional activities. In addition, activins activate ERK signaling and lead to NMDA receptor phosphorylation in neurons. Follistatin specifically binds to activins. The activin-bound follistatin does not have access to ActRIIs. Therefore, follistatins are endogenous inhibitors of activin signals. ActRIIs form large protein complexes, including NMDAR, ARIP1, and PSD95.

recruit and phosphorylate activin type I receptors (ActRIs), termed activin receptor-like kinase 4 (ALK4 also known as ActRIB) for activin A or ALK7 for activin B. Activated ActRIs then phosphorylate transcriptional factors Smad2/3, and phosphorylated Smad2/3 binds to Smad4. Subsequently, Smad complexes are translocated to the nucleus to regulate transcriptional activities. Follistatins, which are also secreted factors, bind to activins with high affinity. The activin-bound follistatin does not have access to activin receptors (Fig. 9.1). Therefore, follistatins are specific inhibitors for the activin-signaling cascade.

Inhibin βA KO mice die within 24 h after birth, and *Follistatin* KO mice exhibit growth retardation and die within hours after birth, which is due to respiratory failure (Matzuk *et al.*, 1995a,b), demonstrating that activin signals are important for normal embryonic and postnatal development. Activin signals are also involved in the pathogenesis of a variety of diseases, including metabolic diseases, musculoskeletal disorders, cancers, and mental disorders. According to recent studies, activin signaling could be a promising target for these disorders (Tsuchida *et al.*, 2009).

Recently, we generated several types of transgenic mice, which demonstrated that activins regulate spine formation, behavioral activity, anxiety, adult neurogenesis, late-phase long-term potentiation (LTP), and maintenance of long-term memory (LTM). This chapter provides an overview of recent progress in the study of the role of activin in the brain.

II. Expression Pattern of Activin and Activin Receptor in the Brain

In 1995, Andreasson and Worley isolated the neural activity-dependent gene *inhibin* βA mRNA and showed that its regulation was dependent upon *N*-methyl-D-aspartate (NMDA) receptor activation (see Section III about NMDA receptor; Andreasson and Worley, 1995). At the same time using the differential display method, *inhibin* βA mRNA was identified as a neural activity-dependent gene in the rat hippocampus (Inokuchi *et al.*, 1996). In contrast, however, *inhibin* α mRNA levels were not affected by neuronal activity (Inokuchi *et al.*, 1996). In addition, activin receptor *ActRII* mRNA is expressed in the adult brain and is specifically abundant in the hippocampus and amygdala (Cameron *et al.*, 1994). Immunohistochemical analysis also revealed ActRII expression in neurons of the cerebral cortex, hippocampus, medial amygdala, and thalamus (Funaba *et al.*, 1997).

III. Activin Receptor and its Regulatory Proteins

The brain is composed of neurons that communicate with one another by transmitting chemicals (neurotransmitters) (Fig. 9.2A). To accomplish this, neurons develop two distinct processes—axons and dendrites (Fig. 9.2A). Information flows from one neuron to another across a synapse, which is a small gap between the neurons. Chemicals (neurotransmitters) are released from the axonal terminal (presynapse), which then bind to cell-surface receptors located on the dendrites (postsynapse; Fig. 9.2A). Spines are small, membranous protrusions on the dendrite. The majority of spines have a bulbous head (the spine head) and a thin neck that connects the head of the spine to the dendrite shaft (Fig. 9.2A). In the spine head, crucial proteins accumulate to respond to presynaptic regional signals, which are linked by scaffold proteins.

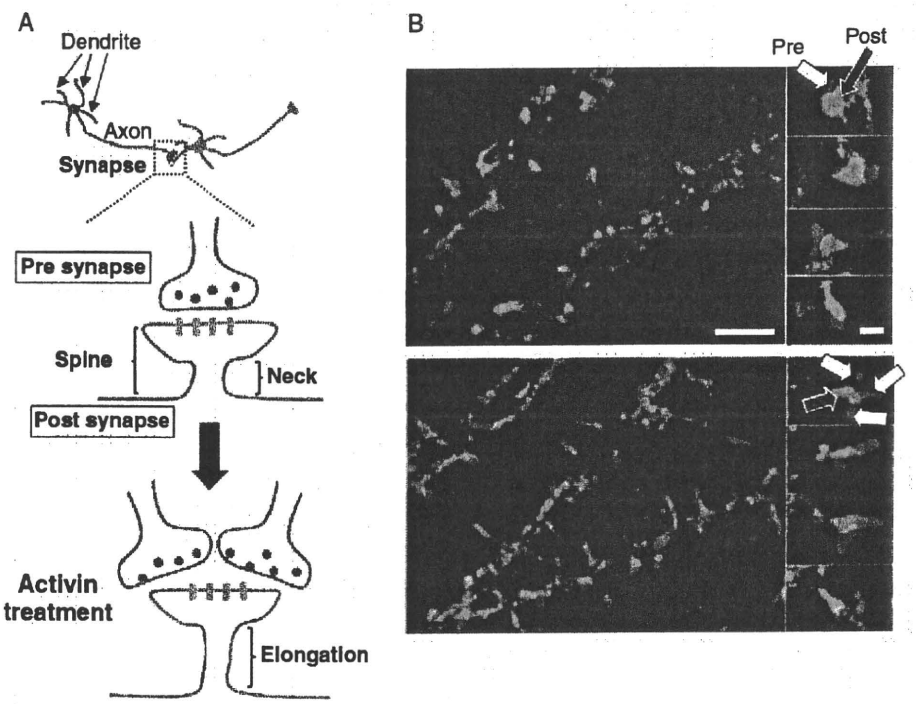

Figure 9.2 Activins regulate spine morphology. (A) Illustration of neuron, synapse, and spine structures. (B) Cultured hippocampal neurons were treated with vehicle (upper) and activins (lower), followed by staining with phalloidin to identify F-actin (red, blue arrows) and antisynaptophysin antibody (green, white arrows) to identify presynaptic regions. Scale bar, 1 μm.

Activin type II receptor, ActRII, binds to a scaffold protein called activin receptor interacting protein 1 (ARIP1)/synaptic scaffolding molecule (S-SCAM)/membrane-associated guanylate kinase, WW and PDZ domain containing 2 (MAGI2), which is localized at the postsynaptic site (Fig. 9.1). In addition, ARIP1 binds to guanylate kinase domain-associated protein (GKAP), Fyn kinase (Kurisaki *et al.*, 2008), and Smad3 (Shoji *et al.*, 2000). Postsynaptic density 95 (PSD95) is a well-characterized scaffold protein in the postsynaptic region, which binds to various protein types, including channel/receptor proteins (e.g., K channel, NMDA receptor, and Erb4), adhesion proteins (e.g., neuroligin), signaling proteins (e.g., synaptic RasGAP (SynGap) and neuronal nitric oxide synthase (nNOS)), and other neuronal function regulators (e.g., Stargazin and GKAP; Hata and Takai, 1999; Sheng and Sala, 2001; Talmage, 2008). GKAP binds to numerous proteins *via* Shank (Tu *et al.*, 1999) and Vesl-1L/Homer-1C (Kato *et al.*, 1998). Therefore, ActRII is a component of the huge PSD-95 protein complex located in the postsynaptic site.

Glutamate is the major excitatory neurotransmitter in the mammalian central nerve system (CNS). It acts *via* two classes of receptors—ligand-gated ion channels (ionotropic receptors) and G-protein-coupled metabotropic receptors. The ionotropic glutamate receptors are subdivided into three groups (AMPA, NMDA, and kainate receptors) based on pharmacological properties. NMDA receptors are highly expressed in the hippocampus, and dysregulated activation and/or inhibition of NMDA receptors influences many CNS disorders, including stroke, Parkinson's disease, Alzheimer's disease, epilepsy, drug dependence, depression, anxiety, and schizophrenia (Muir, 2006; Parsons *et al.*, 1999; Sawa and Snyder, 2002; Skolnick, 1999). Activation of NMDA receptors results in influx of Ca^{2+}. Ca^{2+} influx through NMDA receptors is thought to play critical roles for memory acquisition and LTP (see Section IV.D for details).

Activin treatment induces phosphorylation of NMDA receptors in primary hippocampal cultures, which is dependent on Fyn tyrosine kinase and ARIP1. In addition, activins increase Ca^{2+} influx through these NMDA receptor complexes (Kurisaki *et al.*, 2008). These results indicate that activins influence neuronal activity and are involved in a multitude of CNS disorders. According to our recent work, activins also play a role in anxiety, memory, and LTP (see below).

IV. Functions of Activins in the CNS

A. Activin regulates spine formation

Individual spines, which are comprised of cytoskeletal actin, undergo actin-dependent shape changes that are regulated by neurotransmitter stimulation. This phenomenon could contribute to plasticity of brain circuits (Fischer *et al.*, 1998, 2000; Fukazawa *et al.*, 2003; Honkura *et al.*, 2008; Matus, 2005).

In typical hippocampal cultures, the majority of spine contact takes place at only one presynaptic site. Activin treatment enhances the number of presynaptic contacts per individual spine, which elevates the average length of the spine neck through F-actin organization (Fig. 9.2B; Shoji-Kasai *et al.*, 2007).

In addition to the canonical Smad pathway, activin receptors activate other Smad-independent pathways (p38 MAPK, ERK1/2, and JNK) in a cell type-specific manner (Bao *et al.*, 2005; de Guise *et al.*, 2006; ten Dijke *et al.*, 2000; Werner and Alzheimer, 2006). The influence of activins on spinal morphology is independent of protein and RNA synthesis (Shoji-Kasai *et al.*, 2007). However, it is interesting to note that these phenomena are completely blocked by treatment with MEK inhibitor. Following treatment with activins, ERK1/2 phosphorylation is markedly increased in hippocampal cultures, but not in astroglial-enriched cultures. However, activins do not result in a significant increase in JNK and p38 MAPK phosphorylation. These results suggested that ERK pathways primarily affect activin-dependent spine changes in hippocampal neurons.

B. Activin influences depression and anxiety-related behavior

Mood disorders, such as bipolar disorder and depression, represent one of the most common mental illnesses, affecting as many as 17% individuals in the United States (Kessler *et al.*, 1994). Because depression is a leading cause of suicide, it is considered a serious disorder in today's society.

Previous results have shown that activin A infusion into the rat hippocampus produced an antidepressant-like effect in the forced swimming test, which is typically used to assess the effects of antidepressant drugs (Dow *et al.*, 2005).

We have generated activin and follistatin transgenic mice under the control of the αCaMKII promoter, whose activity is thought to influence postnatal development in the forebrain. Several behavioral analyses were performed on these mice—namely, open field test, light and dark choice test, elevated plus maze test, and novel-area accessing test (Ageta *et al.*, 2008). The open field test is used to measure locomotor activity, and light and dark choice test, elevated plus maze test, and novel-area accessing test are used to measure anxiety levels. Results demonstrated that follistatin overexpression mice (FSM) exhibit decreased general locomotor activity and enhanced anxiety. In contrast, activin overexpression mice (ACM) exhibit more aggressive behavior than wild-type littermates, as well as reduced anxiety-related behavior. These results showed that activin levels in the forebrain affect locomotor activity and anxiety-related behavior (Fig. 9.3 and Table 9.1).

Other studies have generated dominant-negative ActRIB transgenic mice under control of the αCaMKII promoter, which demonstrated that activin signals are negative regulators of anxiety (Zheng *et al.*, 2009). For

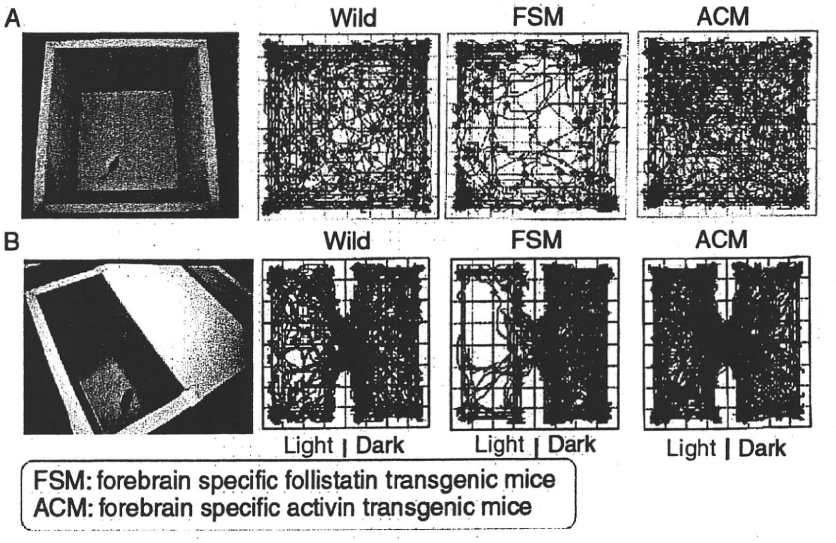

Figure 9.3 Activins influence anxiety-related behavior. (A) Open field test. (B) Light and dark test. Right panels show typical traces for each genotype.

example, these mice visited a greater number of inner fields in the open field test, which represents risk-taking behavior, and the mice also spent more time on lit, elevated places in the light-dark exploration test. These behaviors correlate with the level of anxiety in an animal, and results from this study were consistent with results from our laboratory. However, the conflicting results between the two studies could be due to transgene differences; Zheng *et al.* utilized the dominant-negative receptor ActRIB as a transgene. By contrast, we have utilized secreted factors (activins and follistatins) to determine the role of activin in the brain. GDF11, another member of the TGF-β superfamily, is expressed in the adult brain and it also binds to activin receptor II and IB. (Nakashima *et al.*, 1999). Therefore, differences in results could be due to regulation of GDF11, as well as activins. It is possible that the dominant-negative receptor ActRIB dimerizes with receptors of the TGF-β family members other than activins.

Alternatively, the dominant-negative ActRIB lacks a cytoplasmic kinase domain, thereby blocking the activin-Smad signaling cascade (see above, Fig. 9.1). Recent studies have shown that Smurf1, an E3 ubiquitin ligase, associates with the cytoplasmic domain of the TGF-β type I receptor and induces internalization and degradation of TGF-β receptors (Di Guglielmo *et al.*, 2003; Ebisawa *et al.*, 2001; ten Dijke and Hill, 2004). ActRIB also binds to and is ubiquitinated by the Smad7–Smurf1 complex *via* the ActRIB cytoplasmic domain (Yamaguchi *et al.*, 2006). Furthermore, activin-dependent spine changes are independent of Smad activation in hippocampal cultures (Shoji-Kasai *et al.*, 2007) (see above, Fig. 9.2). *In vivo*, if activin receptors are regulated by this kind of ubiquitination and proteasomal degradation,

Table 9.1 Summary of behavioral analysis of FSM and ACM

	Open field test				Light and dark test	Elevated plus-maze test	Novel-area accessing test
	Walking speed	Time spent in locomotion	Time in rearing	Risk-taking behavior	Time in light compartment	Time in open arm	Time in novel area
FSM	–	↓	↓	↓	↓	–	↓
ACM	–	–	↑	↑	↑	↑	NT

↓ downregulated compared with wild-type mice; ↑ upregulated compared with wild-type mice; – not significant change in behavior; NT, not tested; ACM, forebrain-specific activin transgenic mice; FSM, forebrain-specific follistatin transgenic mice.